Polarization near Dislocation Cores in $SrTiO_3$ Single Crystals: The Role of Flexoelectricity

Xiaoxing Cheng,[1,a)] Bo Wang,[1] and Long-Qing Chen[1,b)]
Material Science and Engineering, The Pennsylvania State University, University Park, Pennsylvania, 16802, United States of America

(Dated: 17 March 2024)

Spontaneous polarization as large as $\sim 28\ \mu C/cm^2$ was recently observed around the dislocation cores in non-polar $SrTiO_3$ bulk crystals, and its origin was attributed to the flexoelectric effect, i.e., polarization induced by strain gradients. However, the roles of flexoelectricity, relative to other electromechanical contributions, and the nature of dislocations, i.e. edge versus screw dislocations in the induced polarization are not well understood. In this work, we study the role of flexoelectricity in inducing polarization around three types of dislocation cores in $SrTiO_3$: $b = a(100)$ edge dislocation, $b = a(110)$ edge dislocation, and $b = a(010)$ screw dislocation, where b is the Burgers vector. For the edge dislocations, polarization can be induced by electrostriction alone while flexoelectricity is essential for stabilizing the symmetric polarization pattern. The shear component of the flexoelectric tensor has a dominant effect on the magnitude and spatial distribution of the flexoelectric polarization. In contrast, no polarization is induced around the $b = a(010)$ screw dislocation through either electrostriction or flexoelectricity. Our findings provide an in-depth understanding of the role of flexoelectricity in inducing polarization around dislocation cores and offer insights to the defect engineering of dielectric/ferroelectric materials.

a) Current affiliation: Shenzhen Research Institute of Big Data, Guangdong, 518045, China
b) Author to whom correspondence should be addressed: lqc3@psu.edu.

Main text

$SrTiO_3$ is a quantum paraelectric material that undergoes a transition from cubic to tetragonal in its bulk single-crystal form upon cooling below the antiferrodistortive transition temperature of 105 K. Its transverse optical mode softens near 0 K, although no ferroelectric transition is observed[1–4]. However, ample experimental evidence exists that ferroelectricity can be induced in $SrTiO_3$ through methods such as non-stoichiometry[5,6], strain engineering[7–10], and isotope substitution[11].

Recently, polar regions are observed around $SrTiO_3$ dislocation cores[12], and their appearance is attributed to flexoelectricity, a coupling effect between polarization and strain gradient[13–15]. As a 4th rank tensor, flexoelectricity is present in crystals of all symmetries, unlike piezoelectricity, which is absent in centrosymmetric materials. Although a universal property, the flexoelectric coupling effect is expected to manifest itself only in materials of large dielectric permittivity and under sufficiently large strain gradients[15–20]. In some ferroelectric thin film systems[21,22], researchers have observed strain gradient up to 10^6 /m, which is large at long-scale but not enough to induce flexoelectric polarization. The locally distorted regions around dislocation cores are known to possess large strain gradients, which can reach up to approximately 10^8 /m as shown in our simulation, and may give rise to flexoelectric polarization. However, it is known that other electromechanical coupling effects, such as electrostriction, can also stabilize ferroelectric phases[23,24]. For ferroelectric materials, it is well-known that dislocations influence the polarization domain structure[25,26]. However, it is extremely challenging, if not possible to explicitly separate the contributions of spontaneous polarization, electrostriction, piezoelectricity, and flexoelectricity to the total polarization through experiments. Therefore, using a dielectric material like $SrTiO_3$ as a model system is desirable because it allows us to ignore the contribution of spontaneous polarization and piezoelectricity since bulk $SrTiO_3$ is not ferroelectric/piezoelectric at room temperature. In this work, we use phase-field simulations to investigate the contributions of flexoelectricity and electrostriction to polarization around dislocation cores in bulk single-crystal $SrTiO_3$. Our phase-field ferroelectric model provides a self-consistent way to isolate and compare the relative contributions of each flexoelectric component.

It is worth noting that the presence of dislocations in $SrTiO_3$ itself may generate a number of complex phenomena[27] such as the interaction of dislocation cores with oxygen vacancies[28–30], the stabilization of local polarization at and near dislocation cores[12], the dislocation reactions and dynamics[31–33]. In this work, we focus on the mechanical ef-

Main text

fect arising from the presence of three common types of dislocations, the $b = a(100)$ edge dislocation, which is widely observed at small angle grain boundaries[12,30] or in plastically deformed crystals at high temperature[34–36], the $b = a(110)$ edge dislocation, and $b = a(010)$ screw dislocation, which are commonly observed in $SrTiO_3$ that undergoes plastic deformation at low temperature[34,35,37]. The polarization and local strain distributions around the $b = a(100)$ edge dislocation have already been characterized in the literature using high-resolution STEM[30] , providing comparisons for the $b = a(100)$ edge dislocation results of Four phase-field calculations.

For all three types of dislocations, only one single dislocation is introduced in all cases. In the real world, however, $b = a(110)$ edge dislocation may dissociate into a pair of partial dislocations, but that is beyond the discussion of this paper. We also recognize that the dislocation core may be charged, which definitely will influence the local polarization distribution. The effect of charges at the dislocation core on the local polarization will be addressed in a future publication.

The phase-field method is employed to simulate the polarization evolution of bulk $SrTiO_3$ in the presence of dislocations[23,38]. The temporal evolution of local polarization and oxygen octahedral tilt can be described by the time-dependent Ginzburg Landau (TDGL) equation (S1) with two sets of order parameters P, the polarization, and Q, the oxygen octahedral tilt. Detailed forms for each free energy term are presented in Equation S3 to S7 of the supplementary material. Comparisons between the numerical and analytical stress distributions are shown in Figure S1. The strain distributions for all three types of dislocations are shown in Figure S2.

A self-consistent steady-state order parameter distribution can be obtained through the coupled solution of TDGL equation (S1), mechanical equilibrium equation (S8), and Poisson equation (S9). All coefficients are listed in the supplementary material table (S1), which are the same as in reference[39]. More details of the simulation setup and how we choose the flexoelectric coefficients for all cases are explained in Figure S3.

Figure 1 shows the stress distribution and strain gradient distribution around $b = a(100)$ edge dislocation. σ_{11} has the largest magnitude because it is directly affected by the dislocation eigenstrain due to the additional atomic plane inside the dislocation loop. Electrostriction, as a quadruple relationship between strain and polarization, can affect the shape of total free energy in Equation S2, and thus equilibrium polarization value[40]. This is illustrated

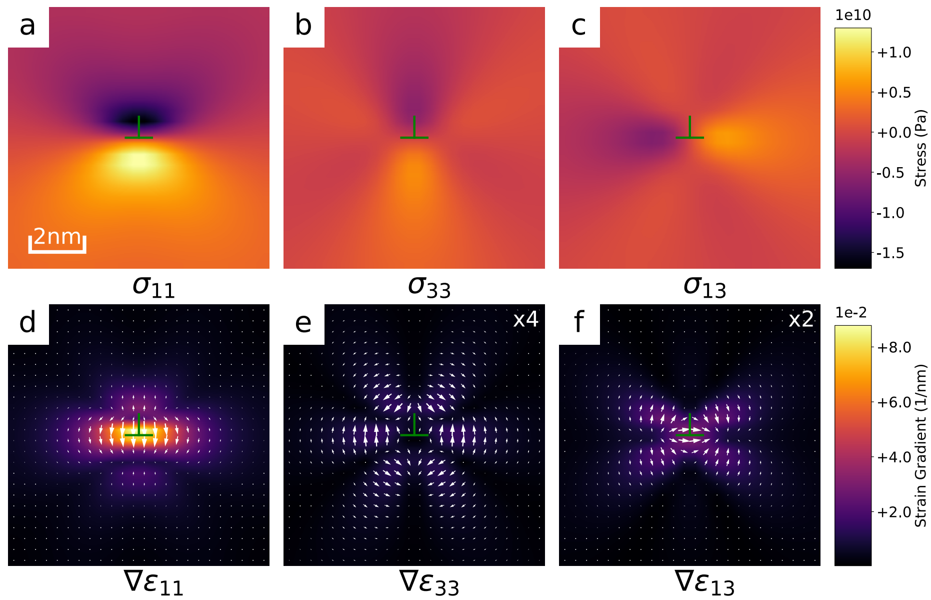

FIG. 1. Stress and strain gradient distributions around $b = a(100)$ edge dislocation core. Background color shows the magnitude of the corresponding data, (a) σ_{11}, (b) σ_{33}, (c) σ_{13}, (d) $\nabla\epsilon_{11}$, (e) $\nabla\epsilon_{33}$, (f) $\nabla\epsilon_{13}$. Subscript 1 means the horizontal axis to the right, subscript 3 means the vertical axis to the up, and the y axis is pointing into the paper. The dislocation core is located at the center of the region marked by the green T. White arrows in (d), (e), and (f) is the gradient vector with scaling factor shown at the top right corner.

in Figure S4 that a moderate tensile stress leads to the ferroelectric phase with polarization along the tensile direction, while compressive stress still leads to the paraelectric phase. The flexoelectric effect, on the other hand, correlates the polarization orientation to the strain gradient, which breaks the central symmetry and stabilizes the ferroelectric phase directly.

The strain gradient distribution in Figure 1(d), (e), and (f), shows that the gradients of ϵ_{11} and ϵ_{33} are mainly along (001) direction while ϵ_{13} gradient is along (100) direction. Additionally, the ϵ_{11} gradient has the largest magnitude, nearly three times those of ϵ_{33} and ϵ_{13}. To activate the flexoelectric effect, a significant strain gradient and a large flexoelectric coefficient are two necessities. Since $\epsilon_{11,3}$ dominates among all strain gradients in the $b = a(100)$ edge dislocation case, according to the relationship $E_3^{flexo} = V_{3333}\epsilon_{33,3} + V_{3311}\epsilon_{11,3} + 2V_{3113}\epsilon_{13,1}$, the flexoelectric field along the z-direction has the largest value, thus we will naturally expect the polarization to be along the z-direction. Surprisingly, the simulation results prove our intuition wrong, the reason for which will become clear as we discuss the results in Figure 2 and 3.

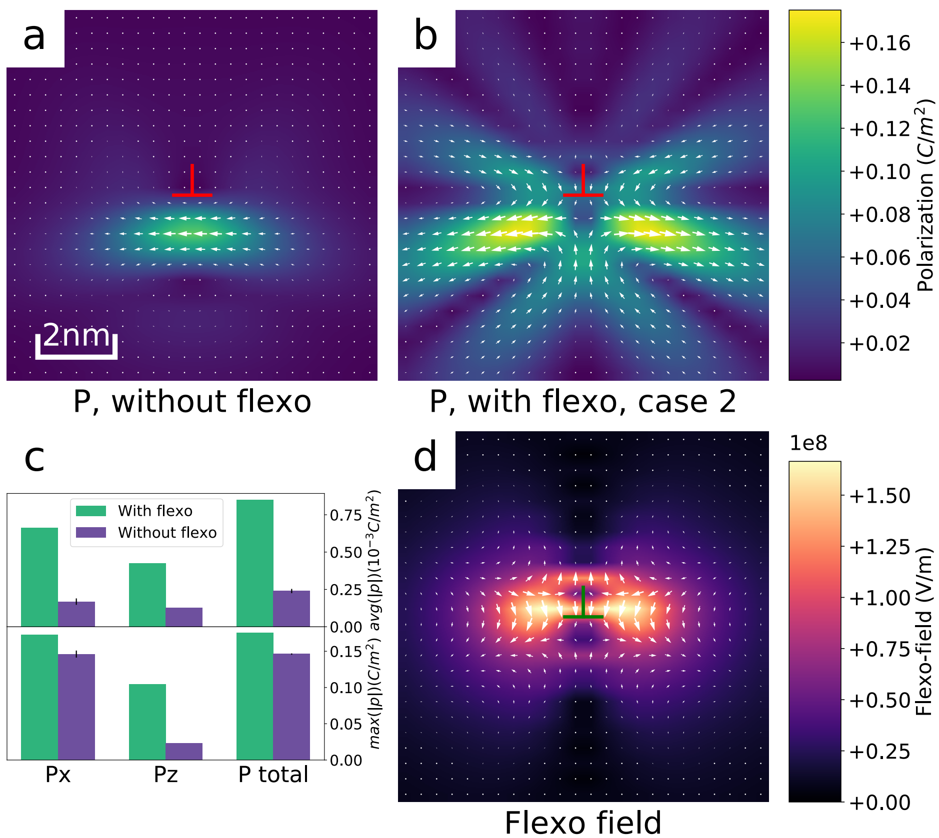

FIG. 2. Comparison of polarization distributions with and without flexoelectric effect. (a) Polarization distribution without flexoelectricity. (b) Polarization distribution considering flexoelectricity, $V_{1111} = 0.08$ V, $V_{1122} = 2.6$ V, $V_{1212} = 2.2$ V. The quivers in (a),(b) indicate the polarization vector and the background heat plot illustrates the magnitude of polarization. (c) Statistics of the average and maximum Px, Pz, and P total. (d) Flexoelectric field distribution, quivers indicate the flexoelectric field and the background heat plot shows the magnitude of the flexoelectric field.

The polarization distributions with and without the flexoelectric contribution are shown in Figure 2. The result in Figure 2(a) is consistent with the analysis in Figure 1(a) and

Figure S4(b,c) that when considering only electrostriction, it is possible to stabilize the polar state in the tensile region below the dislocation core with the polarization orienting along the tensile stress direction, while the material remains in the paraelectric phase in the compressive region above the dislocation core. The reason why the polarization in Figure 2(a) is pointing towards the left is merely due to the initial random noise. We have also observed the other degenerate state with polarization pointing towards the right if starting from a different initial noise. Figure 2(b) shows that when flexoelectricity is taken into consideration (case 2 setup), the polarization becomes mirrored with respect to the z-axis. The flexoelectric field in Figure 2(d) demonstrates more clearly the symmetric relationship of the flexoelectric driving force for polarization around the dislocation core. However, the final polarization distributions are totally different from the flexoelectric field, indicating that though there is a significant change in polarization pattern when flexoelectricity is considered, the electrostrictive effect still plays an important role in determining the final polar state in Figure 2(b). We can draw the same conclusion based on the fact that the polarization distributions in Figure 2(b) have a much larger magnitude in the tensile region below the defect compared to the compressive region above the dislocation. The bar plot in Figure 2(c) shows that flexoelectricity significantly boosts the average polarization magnitude within the plotted region because the "with flexoelectricity" case shows a much larger influential region than the "without flexoelectricity" case. On the other hand, flexoelectricity has a limited effect on the value of maximum polarization, since the maximum always appears below the dislocation in the tensile region where the role of flexoelectricity is more of reorienting the polarization that is already stabilized by electrostriction. The large increase in the maximum Pz value is because in the pure electrostriction case the tensile strain along the x-direction suppresses the occurrence of polarization along the z-axis.

To further understand the influence of flexoelectricity, we took advantage of simulation and performed a series of calculations varying the flexoelectric coefficients. Figure 3 shows the polarization and flexoelectric field distributions for three sets of flexoelectric coefficients. Comparing the polarization patterns in Figure 3 (a), (b), and (c) with the ones in Figure 2(a) and (b), we find that Figure 3(c) resembles Figure 2(b), both have the mirrored shape, while Figure 3(a) and (b) roughly maintain the uni-directional distribution as in the "without flexoelectricity" case in Figure 2(a). These results indicate that for the $b = a(100)$ edge dislocation case, V_{1212} plays a more important role in shaping the polarization distribution

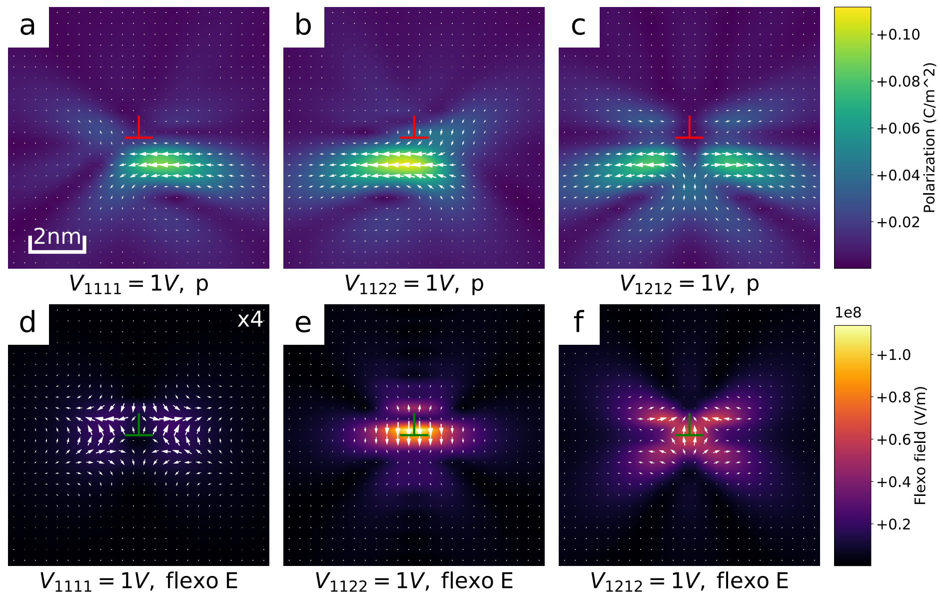

FIG. 3. The polarization and flexoelectric field distributions under different flexoelectric coefficients for $b = a(100)$ edge dislocation. White quiver represents the plotted vector field, and the background heat plot shows the magnitude of the vector. (a, b, c) Polarization distribution. (d, e, f) Flexoelectric field distribution. (a, d) Non-zero longitudinal flexoelectric coefficient. (b, e) Non-zero transverse flexoelectric coefficient. (c, f) Non-zero shear flexoelectric coefficient.

than the other two independent flexoelectric coefficients. As shown in Figure 1 and S5, a non-zero V_{1111} activates $\epsilon_{11,1}$ and $\epsilon_{33,3}$, but because both strain gradients and the coefficient are small, the magnitude of flexoelectric field in Figure 3(d) is small and thus the polarization pattern is only slightly changed compared to the "without flexoelectricity" case. Non-zero V_{1122} value leads to a huge z component in the flexoelectric field due to the large $\epsilon_{11,3}$ value, but such a large driving force does not transform into enhanced polarization along the z-axis. Similar to how strain engineering works in epitaxial thin film, tensile strain favors polarization along the same tensile direction, but not the perpendicular direction[23,40]. While for V_{1212}, the combination of V_{1212} and $\epsilon_{13,3}$ aligns the largest flexoelectric field along the x-direction, as shown in Figure S5, thus stabilizing a symmetric polarization distribution with respect to the dislocation inclusion plane along the x-direction. Some papers suggest that the flexoelectric coefficient may be negative[20,41,42], so we performed several additional simulations with negative flexoelectric coefficients as shown in Figure S6. To make the discussion more complete, Figure S7 shows the case with zero electrostrictive coefficients while maintaining non-zero flexoelectric coefficients.

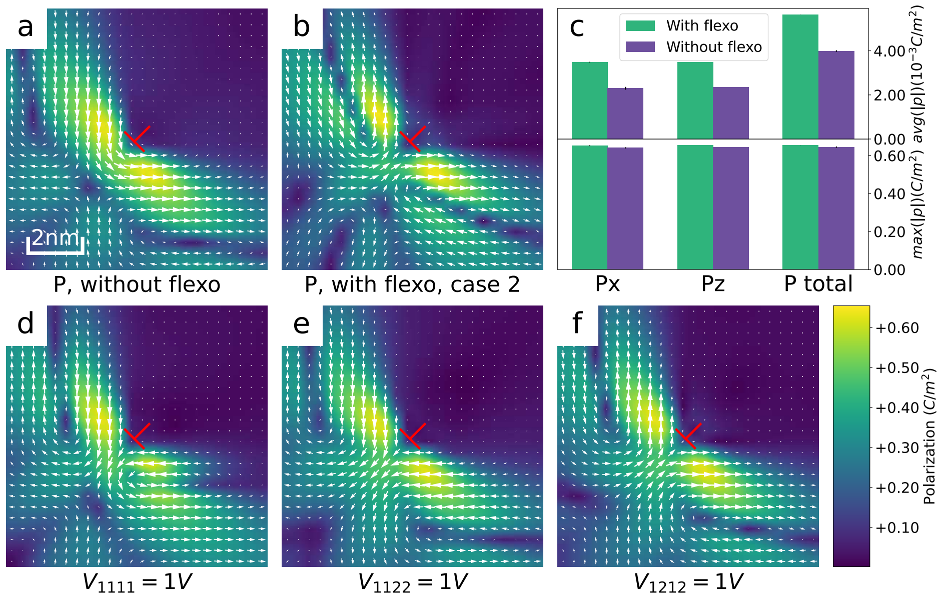

FIG. 4. The polarization distribution under different flexoelectric coefficients for $b = a(110)$ edge dislocation. (a) No flexo. (b) Experimental flexoelectric coefficient $V_{1111} = 0.08$ V, $V_{1122} = 2.6$ V, $V_{1212} = 2.2$ V. (c) Statistics of the average and maximum Px, Pz and P total. (d) Non-zero longitudinal flexoelectric coefficient. (e) Non-zero transverse flexoelectric coefficient. (f) Non-zero shear flexoelectric coefficient.

Next, we perform the same set of calculations and analysis for $b = a(110)$ edge dislocation. In this case, the stress/strain tensor is rotated by 45°, and Burgers vector is longer compared to the $b = a(100)$ edge dislocation, which leads to a larger maximum stress/strain component and a rotated strain gradient vector (see Figure S2 and S8), both have a significant influence on the polarization distribution.

As shown in Figure 4(a), a ferroelectric phase can be stabilized by $b = a(110)$ edge dislocation through the electrostrictive effect alone. It has a much larger polarization magnitude and area compared to the $b = a(100)$ edge dislocation case due to the larger stress/strain values around the $b = a(110)$ edge dislocation core. When flexoelectricity is considered, as shown in Figure 4(b), the flexoelectric field reshapes the polarization into a roughly symmetric pattern with respect to the dislocation inclusion plane. The bar plot in Figure 4(c) displays the average and the maximum polarization magnitudes within the plotted region. We observe that, firstly, both the average and maximum values are several times larger than those of the $b = a(100)$ edge dislocation case due to a much larger local stress/strain distribution. Secondly, flexoelectricity can increase the average polarization value, while it has little effect on the maximum polarization.

In Figure S9 and Figure 4 (d), (e), and (f) we isolate the contribution from each of the flexoelectric coefficients. Similar to the $b = a(100)$ edge dislocation case, the shear flexoelectric coefficient has the most significant influence on polarization distributions. In all cases, the polarization is stabilized and aligned predominantly along the tetragonal directions. The electrostrictive effect primarily stabilizes the polarization by shaping the free energy profile into a double well configuration, which determines the permissible polarization directions (e.g., px+ or px-, with no inherent preference) and its magnitude. Flexoelectricity's principal impact resembles that of an electric field which tilts the free energy profile, forcing the polarization to align with the flexoelectric field. The results for $b = a(010)$ screw dislocation show that neither electrostriction nor flexoelectricity can stabilize any polar state, more details are discussed in Figure S10.

In this study, we explore the role of flexoelectricity in inducing polarization around three types of dislocation cores in bulk $SrTiO_3$, $b = a(100)$ edge dislocation, $b = a(110)$ edge dislocation, and $b = a(010)$ screw dislocation. The effects of electrostriction and flexoelectricity are compared and contributions from the longitudinal, transverse, and shear flexoelectric coefficients are also discussed. Our findings reveal that for both edge dislocation cases, electrostriction alone is sufficient to stabilize the spontaneous polarization within the tensile region by creating the double well free energy profile. The primary role of flexoelectricity is to align the polarization with the flexoelectric field, taking into account the restrictions of the stabilized polarization directions. This leads to a symmetric polarization distribution with respect to the dislocation inclusion plane. Consequently, it is the synergistic influence of both flexoelectricity and electrostriction that determines the final polarization pattern. Polarization values as large as 0.18 C/m^2 and 0.66 C/m^2 are obtained for the $b = a(100)$ edge dislocation and $b = a(110)$ edge dislocation cases respectively, when considering the flexoelectric effect. Our study identifies that the shear component of the flexoelectric tensor is predominantly responsible for the polarization induced around the dislocation core. Additionally, for the $b = a\langle 010\rangle$ screw dislocations, neither electrostriction nor flexoelectricity can stabilize any polar phase.

The simulations in this work largely corroborate the existing experimental observations of $b = a\langle 100\rangle$ edge dislocation by explicitly analyzing the contributions of flexoelectricity and electrostriction. We predict the polarization patterns around $b = a\langle 110\rangle$ edge dislocation and the absence of polarization in $b = a\langle 010\rangle$ screw dislocation, both of which await validation through future experimental endeavors. Several topics require further investigation. Firstly, our results for oxygen octahedral tilt are 0 at the dislocation core, which is a natural outcome based on the current Landau parameters, but this does not compare well with experimental results. Secondly, the effect of defect charges on the polarization distribution at the dislocation core demands further study. Lastly, the interaction of multiple dislocations in $SrTiO_3$ and its impact on the domain pattern requires a comprehensive examination.

SUPPLEMENTARY MATERIAL

The supplementary material includes a detailed description of the phase-field model, along with additional figures to complement our discussions.

ACKNOWLEDGEMENTS

X.X.C. and L.-Q.C. were supported by the U.S. Department of Energy, Office of Basic Energy Sciences, under Award DE-SC0020145. B.W. was partially supported by the National Science Foundation (NSF) grant number DMR-1744213 and DMR- 2133373. Computations for this research were performed on the Roar supercomputer at the Institute for Computational and Data Sciences supercomputer of the Pennsylvania State University. All simulations in this study were conducted using the commercial ferroelectric phase-field simulation software from Mu-PRO LLC.

REFERENCES

[1] R. C. Neville, B. Hoeneisen, and C. A. Mead, "Permittivity of Strontium Titanate," Journal of Applied Physics **43**, 2124–2131 (1972).

Main text

[2]K. A. Müller and H. Burkard, "$SrTiO_3$: An intrinsic quantum paraelectric below 4 K," Physical Review B **19**, 3593–3602 (1979).

[3]H. Unoki and T. Sakudo, "Electron Spin Resonance of Fe^{3+} in $SrTiO_3$ with Special Reference to the 110K Phase Transition," Journal of the Physical Society of Japan **23**, 546–552 (1967).

[4]P. A. Fleury, J. F. Scott, and J. M. Worlock, "Soft Phonon Modes and the 110K Phase Transition in $SrTiO_3$," Physical Review Letters **21**, 16–19 (1968).

[5]H. W. Jang, A. Kumar, S. Denev, M. D. Biegalski, P. Maksymovych, C. W. Bark, C. T. Nelson, C. M. Folkman, S. H. Baek, N. Balke, C. M. Brooks, D. A. Tenne, D. G. Schlom, L. Q. Chen, X. Q. Pan, S. V. Kalinin, V. Gopalan, and C. B. Eom, "Ferroelectricity in Strain-Free $SrTiO_3$ Thin Films," Physical Review Letters **104**, 197601 (2010).

[6]D. A. Tenne, A. K. Farrar, C. M. Brooks, T. Heeg, J. Schubert, H. W. Jang, C. W. Bark, C. M. Folkman, C. B. Eom, and D. G. Schlom, "Ferroelectricity in nonstoichiometric $SrTiO_3$ films studied by ultraviolet Raman spectroscopy," Applied Physics Letters **97**, 142901 (2010).

[7]J. H. Haeni, P. Irvin, W. Chang, R. Uecker, P. Reiche, Y. L. Li, S. Choudhury, W. Tian, M. E. Hawley, B. Craigo, A. K. Tagantsev, X. Q. Pan, S. K. Streiffer, L. Q. Chen, S. W. Kirchoefer, J. Levy, and D. G. Schlom, "Room-temperature ferroelectricity in strained $SrTiO_3$," Nature **430**, 758 (2004).

[8]M. D. Biegalski, E. Vlahos, G. Sheng, Y. L. Li, M. Bernhagen, P. Reiche, R. Uecker, S. K. Streiffer, L. Q. Chen, V. Gopalan, D. G. Schlom, and S. Trolier-McKinstry, "Influence of anisotropic strain on the dielectric and ferroelectric properties of $SrTiO_3$ thin films on $DyScO_3$ substrates," Physical Review B **79**, 224117 (2009).

[9]R. Wördenweber, E. Hollmann, R. Kutzner, and J. Schubert, "Induced ferroelectricity in strained epitaxial $SrTiO_3$ films on various substrates," Journal of Applied Physics **102**, 044119 (2007).

[10]R. Xu, J. Huang, E. S. Barnard, S. S. Hong, P. Singh, E. K. Wong, T. Jansen, V. Harbola, J. Xiao, B. Y. Wang, S. Crossley, D. Lu, S. Liu, and H. Y. Hwang, "Strain-induced room-temperature ferroelectricity in SrTiO3 membranes," Nature Communications **11**, 3141 (2020).

[11]M. Itoh and H. Taniguchi, "Ferroelectricity of SrTiO3 Induced by Oxygen Isotope Exchange," in *Ferro- and Antiferroelectricity: Order/Disorder versus Displacive*, Structure

and Bonding, edited by N. S. Dalal and A. Bussmann-Holder (Springer Berlin Heidelberg, Berlin, Heidelberg, 2007) pp. 89–118.

[12]P. Gao, S. Yang, R. Ishikawa, N. Li, B. Feng, A. Kumamoto, N. Shibata, P. Yu, and Y. Ikuhara, "Atomic-Scale Measurement of Flexoelectric Polarization at $SrTiO_3$ Dislocations," Physical Review Letters **120**, 267601 (2018).

[13]B. Wang, Y. Gu, S. Zhang, and L.-Q. Chen, "Flexoelectricity in Solids: Progress, Challenges, and Perspectives," Progress in Materials Science (2019), 10.1016/j.pmatsci.2019.05.003.

[14]J. Fousek, L. E. Cross, and D. B. Litvin, "Possible piezoelectric composites based on the flexoelectric effect," Materials Letters **39**, 287–291 (1999).

[15]W. Ma and L. E. Cross, "Flexoelectric polarization of barium strontium titanate in the paraelectric state," Applied Physics Letters **81**, 3440–3442 (2002).

[16]P. Zubko, G. Catalan, and A. K. Tagantsev, "Flexoelectric Effect in Solids," Annual Review of Materials Research **43**, 387–421 (2013).

[17]W. Ma and L. E. Cross, "Flexoelectric effect in ceramic lead zirconate titanate," Applied Physics Letters **86**, 072905 (2005).

[18]G. Catalan, A. Lubk, A. H. G. Vlooswijk, E. Snoeck, C. Magen, A. Janssens, G. Rispens, G. Rijnders, D. H. A. Blank, and B. Noheda, "Flexoelectric rotation of polarization in ferroelectric thin films," Nature Materials **10**, 963–967 (2011).

[19]D. Lee, A. Yoon, S. Y. Jang, J.-G. Yoon, J.-S. Chung, M. Kim, J. F. Scott, and T. W. Noh, "Giant Flexoelectric Effect in Ferroelectric Epitaxial Thin Films," Physical Review Letters **107**, 057602 (2011).

[20]T. Xu, J. Wang, T. Shimada, and T. Kitamura, "Direct approach for flexoelectricity from first-principles calculations: Cases for SrTiO3 and BaTiO3," Journal of Physics: Condensed Matter **25**, 415901 (2013).

[21]Y. L. Tang, Y. L. Zhu, X. L. Ma, A. Y. Borisevich, A. N. Morozovska, E. A. Eliseev, W. Y. Wang, Y. J. Wang, Y. B. Xu, Z. D. Zhang, and S. J. Pennycook, "Observation of a periodic array of flux-closure quadrants in strained ferroelectric PbTiO3 films," Science **348**, 547–551 (2015).

[22]Y. L. Tang, Y. L. Zhu, Y. Liu, Y. J. Wang, and X. L. Ma, "Giant linear strain gradient with extremely low elastic energy in a perovskite nanostructure array," Nature Communications **8**, 15994 (2017).

[23] Y. L. Li, S. Choudhury, J. H. Haeni, M. D. Biegalski, A. Vasudevarao, A. Sharan, H. Z. Ma, J. Levy, V. Gopalan, S. Trolier-McKinstry, D. G. Schlom, Q. X. Jia, and L. Q. Chen, "Phase transitions and domain structures in strained pseudocubic (100) $SrTiO_3$ thin films," Physical Review B **73**, 184112 (2006).

[24] K. Masuda, L. Van Lich, T. Shimada, and T. Kitamura, "Periodically-arrayed ferroelectric nanostructures induced by dislocation structures in strontium titanate," Physical Chemistry Chemical Physics **21**, 22756–22762 (2019).

[25] M. Höfling, X. Zhou, L. M. Riemer, E. Bruder, B. Liu, L. Zhou, P. B. Groszewicz, F. Zhuo, B.-X. Xu, K. Durst, X. Tan, D. Damjanovic, J. Koruza, and J. Rödel, "Control of polarization in bulk ferroelectrics by mechanical dislocation imprint," Science **372**, 961–964 (2021).

[26] N. Li, R. Zhu, X. Cheng, H.-J. Liu, Z. Zhang, Y.-L. Huang, Y.-H. Chu, L.-Q. Chen, Y. Ikuhara, and P. Gao, "Dislocation-induced large local polarization inhomogeneity of ferroelectric materials," Scripta Materialia **194**, 113624 (2021).

[27] K. Szot, C. Rodenbücher, G. Bihlmayer, W. Speier, R. Ishikawa, N. Shibata, and Y. Ikuhara, "Influence of Dislocations in Transition Metal Oxides on Selected Physical and Chemical Properties," Crystals **8**, 241 (2018).

[28] W. Jiang, M. Noman, Y. M. Lu, J. A. Bain, P. A. Salvador, and M. Skowronski, "Mobility of oxygen vacancy in $SrTiO_3$ and its implications for oxygen-migration-based resistance switching," Journal of Applied Physics **110**, 034509 (2011).

[29] D. Marrocchelli, L. Sun, and B. Yildiz, "Dislocations in $SrTiO_3$: Easy To Reduce but Not so Fast for Oxygen Transport," Journal of the American Chemical Society **137**, 4735–4748 (2015).

[30] P. Gao, R. Ishikawa, B. Feng, A. Kumamoto, N. Shibata, and Y. Ikuhara, "Atomic-scale structure relaxation, chemistry and charge distribution of dislocation cores in $SrTiO_3$," Ultramicroscopy **184**, 217–224 (2018).

[31] T. Matsunaga and H. Saka, "Transmission electron microscopy of dislocations in $SrTiO_3$," Philosophical Magazine Letters **80**, 597–604 (2000).

[32] Z. Mao and K. M. Knowles, "Dissociation of lattice dislocations in $SrTiO_3$," Philosophical Magazine A **73**, 699–708 (1996).

[33] S. Kondo, T. Mitsuma, N. Shibata, and Y. Ikuhara, "Direct observation of individual dislocation interaction processes with grain boundaries," Science Advances **2**, e1501926

(2016).

[34] P. Hirel, P. Carrez, and P. Cordier, "From glissile to sessile: Effect of temperature on ⟨110⟩ dislocations in perovskite materials," Scripta Materialia **120**, 67–70 (2016).

[35] S. Taeri, D. Brunner, W. Sigle, and M. Rühle, "Deformation behaviour of strontium titanate between room temperature and 1800 K under ambient pressure," Zeitschrift für Metallkunde **95**, 433–446 (2004).

[36] L. Porz, T. Frömling, A. Nakamura, N. Li, R. Maruyama, K. Matsunaga, P. Gao, H. Simons, C. Dietz, M. Rohnke, J. Janek, and J. Rödel, "Conceptual Framework for Dislocation-Modified Conductivity in Oxide Ceramics Deconvoluting Mesoscopic Structure, Core, and Space Charge Exemplified for SrTiO3," ACS Nano **15**, 9355–9367 (2021).

[37] W. Sigle, C. Sarbu†, D. Brunner, and M. Rühle, "Dislocations in plastically deformed SrTiO3," Philosophical Magazine **86**, 4809–4821 (2006).

[38] L.-Q. Chen, "Phase-Field Method of Phase Transitions/Domain Structures in Ferroelectric Thin Films: A Review," Journal of the American Ceramic Society **91**, 1835–1844 (2008).

[39] G. Sheng, Y. L. Li, J. X. Zhang, S. Choudhury, Q. X. Jia, V. Gopalan, D. G. Schlom, Z. K. Liu, and L. Q. Chen, "A modified Landau–Devonshire thermodynamic potential for strontium titanate," Applied Physics Letters **96**, 232902 (2010).

[40] F.-Y. Lin, X. Cheng, L.-Q. Chen, and S. B. Sinnott, "Strain effects on domain structures in ferroelectric thin films from phase-field simulations," Journal of the American Ceramic Society **101**, 4783–4790 (2018).

[41] R. Maranganti and P. Sharma, "Atomistic determination of flexoelectric properties of crystalline dielectrics," Physical Review B **80**, 054109 (2009).

[42] M. Stengel, "Unified ab initio formulation of flexoelectricity and strain-gradient elasticity," Physical Review B **93**, 245107 (2016).